Modeling of Demining Scenarios Using Metal Detectors

John Fernando Vargas Buitrago[#+1], Roberto Bustamante Miller[#2], Mark E. Everett[*3]
Department of Electrical and Electronic Engineering, Universidad de los Andes
Bogotá – Colombia (111711)
+ Faculty of Information and Communications Technology, Universidad Pontificia Bolivariana
Medellín – Colombia (050031)
1. varjof@yahoo.com
2. rbustama@uniandes.edu.co
* Department of Geology and Geophysics, Texas A&M University
College Station, TX – USA (77843)
3. everett@geo.tamu.edu

Abstract— This paper presents an analytical model and a numerical model that uses the finite element method to simulate demining scenarios using metal detectors. Using the analytical model, simulations of typical demining scenarios with varying parameters were executed. In addition, an analysis was made that aids in clearly understanding the effect of the scenario variables on a Continuous Wave metal detector response. In order to experimentally validate the numerical model, a Continuous Wave metal detector prototype was built to obtain experimental data. The numerical method can also be used to simulate demining scenarios with high metallic content landmines.

Keywords: Demining, Electromagnetic modeling, Finite Element Method, Landmines, Metal detectors.

I. INTRODUCTION

Nowadays, buried land mines are considered a problem of high importance in countries such as Afghanistan, Colombia and Cambodia, among others, which continue to claim civilian and military lives. In the fight to eradicate mines, the Colombian army and entities in charge of demining keep metal detectors as the best technology option for detection; even above the most advanced equipment such as Ground Penetrating Radar (GPR). In the execution of mine detection, the metal detector is the most common tool. GPR accompanied by a metal detector (dual sensor) seems to be the most promising technology [1]. Although metal detectors have been used for mines detection for more than sixty years, it is considered that the full potential of metal detectors has not been exploited. This is due to the lack of rigorous three dimensional electromagnetic modeling tools for this type of systems [2] and to the low dissemination of research results by the manufacturer detectors [3].

A pair or rigorous models of the CSEM response of a 3D conductively arbitrary stage, with homogeneous permeability with solution in finite elements, were originally presented by [4] and [5]. The latter is based on a weak formulation of Maxwell diffusion equations using Coulomb- Gauged Potentials; this is a general model that can be applied in areas such as mining, ground water exploration and environmental geophysics [5]. It was implemented, slightly modified, and theoretically and experimentally validated by [6] with the intent to observe the influence of the terrain topology responding to an electromagnetic induction sensor , as well as to observe the influence of mutual coupling between buried metals in the context of detection of unexploded ordnance (UXO).

In the meantime, based on equations previously presented, in [7], they published a 3D analytical model of metal detection stages that was used in [3] in order to analyze the influence of soil properties on metal detectors performance. Although analytical models are less flexible than the numerical techniques, they are valuable tools to start observing the principle of physical functioning problems and their dependence to the parameters of the system [8]. This model was limited to homogeneous soils, concentric transmitter and receiver loops, and a single spherical buried object with the possibility to arbitrarily allocate the electrical conductivity and magnetic permeability of the soil and the buried sphere. Using this model on [3] they concluded that magnetic permeability is the dielectric properties of the soil that affects the performance of metal detectors the most. Additionally, it raised the need to use a model that would simulate buried objects arbitrarily. Also using analytical models, in [8], they made an extensive study about the influence of the soil on the performance of the detectors and the possibilities to counteract its effects keeping the same restrictions used on [3]; the study expressed the need to use models in which soil is not homogeneous.

The fact that the soil is not homogeneous and that buried objects have an arbitrary form, is covered by the model used on [6] however, this model does not allow assigning a magnetic permeability neither to the soil nor to buried objects different than vacuum permeability. A novel evolution of this model which allows assigning varying magnetic permeability to soil and buried objects was presented a few years ago by [9]. In this model the

edge based finite element method (FEM) is used to solve the Maxwell diffusion equations in Ungauged coupled-potentials formulation; this model was developed in order to make a better interpretation of the data taken in geophysical applications in the presence of buried structures as tunnels, storage tanks or unexploded ordnance structures. The model was theoretically validated against analytical solutions and against other numerical solutions but an experimental validation has not been done. This study intends to show some results using the model presented in [7] to get a better knowledge of the physical phenomena present in metal detection and to demonstrate that the finite element model of [9] is applicable to simulate demining scenarios, by doing an experimental validation using a continuous wave metal detector laboratory prototype.

II. MODELING OF METAL DETECTORS

A metal detector model must represent a typical demining scenario that includes a circular or rectangular transmitter coil, supplied with a time varying current, a homogenous or layered soil with electrical conductivity "σ_{soil}" and permeability "μ_{soil}", one or many metallic buried objects with conductivity "σ_{target}" and permeability "μ_{target}" (Fig 1), and one or many receiver coils located at different places to calculate the induced electromagnetic field or voltage.

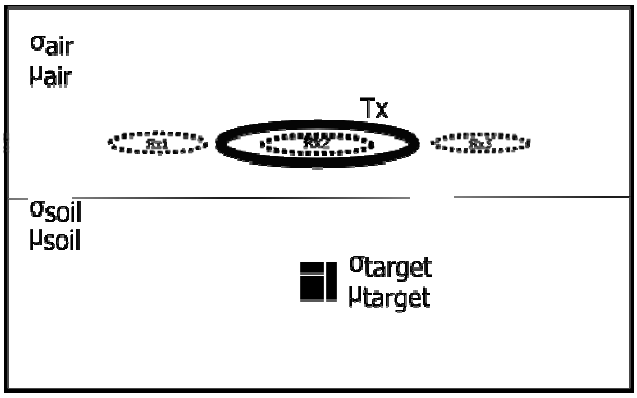

Fig 1. Demining scenario

Metal detector used in demining use the principle of electromagnetic induction, under this principle, the transmitter coil generates a varying electromagnetic field that induces currents in the buried objects; these currents generate electromagnetic fields which can be sensed by the receiver coils.

Continuous Wave (CW) method (frequency domain) and Pulse Induction (PI) method (time domain) are the most common methods used in commercial detectors[10], these methods use varying electromagnetic fields generated by currents such as those shown in Fig 2. In CW method, the magnitude and phase of the electromagnetic field sensed by de receiver depends on the permeability and conductivity of soil and buried objects [6]. In PI method, the magnetic field generated by the buried metal decays in time depending on the characteristics of the object, and its change rate is measured by the receiver.

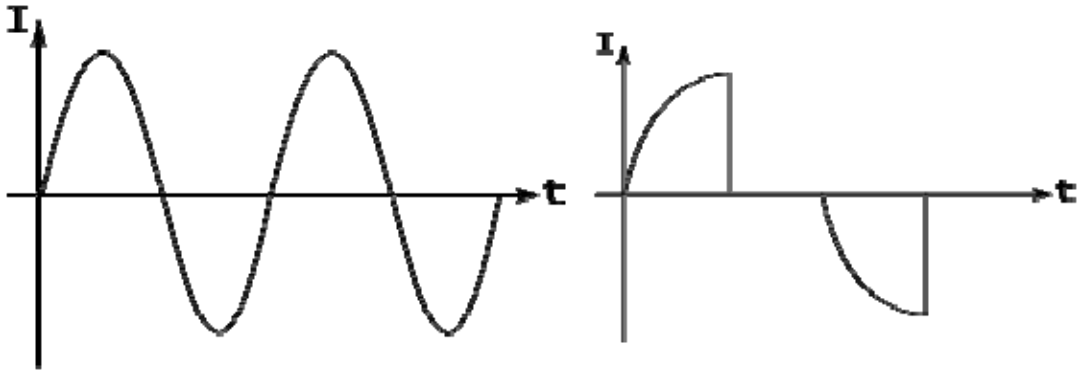

Fig 2. Current shape in Continuous Wave and Pulse Induction metal detectors

The induction phenomena is described by Maxwell equations [11]

$$\nabla \times H(\omega) = \sigma(r)E(\omega) + J_P(\omega) + i\omega\varepsilon E(\omega) \quad (1)$$

$$\nabla \times E(\omega) = -i\omega\mu H \quad (2)$$

$$\nabla \cdot H(\omega) = 0 \quad (3)$$

$$\nabla \cdot E(\omega) = \frac{\rho}{\varepsilon} \quad (4)$$

Where E(V/m) is electric field, H(A/m) is magnetic field, ω(rad) is angular frequency, μ(H/m) is magnetic permeability, σ(S/m) is electrical conductivity, ε(F/m) is electric permittivity and $J_P(A/m^2)$ is the source current density that varies sinusoidally ($J_P= J_o e^{i\omega t}$).

Since that the highest transmitted frequency in metal detectors is usually 50 KHz [7] and the soil's conductivities are below 1 S/m and the permittivity is in the order of 10^{-11}F/m, it is satisfied that: $\omega\epsilon/\sigma \ll 1$, according to this, the displacement current ($i\omega\varepsilon E(\omega)$) is very low compared to the conduction current ($\sigma(r)E(\omega)$), and the present electromagnetic phenomenon is not a wave propagation phenomenon, but a diffusion phenomenon inside the earth. Therefore, it is possible to model the system with the Maxwell diffusion equations, (1) becomes (5), and soil or metal's electric permittivity is irrelevant.

$$\nabla \times H(\omega) = \sigma(r)E(\omega) + J_P(\omega) \qquad (5)$$

A. Analytical Model of a Metal Detection Scenario

This model corresponds to the compilation of equations made in [7]. The modeled scenario includes a transmitter coil feed with a sinusoidal time variable current (Continuous Wave Detector) a concentric with the transmitter receiver coil, a flat and homogeneous soil with arbitrary electrical conductivity "σ_{soil}" and magnetic permeability "μ_{soil}", and a metallic buried sphere, located at depth "d" and distance "ρ_o" from the loop axis (Fig 3).

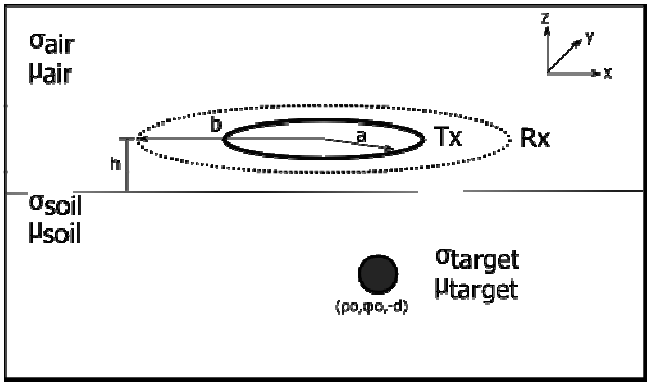

Fig 3. Modeled system

This model allows calculating the induced voltage in the receiver coil by the transmitter (V_{air}), by the soil (V_{soil}) and by the buried object (V_{target}).

1) Induced Voltage in the Receiver by the Transmitter and the Soil:

The voltage induced by the coil transmitter and by the soil in a receiver coil of radius "b", and Nr turns, concentric with the transmitter and placed at the same height is:

$$V^{air} = \pi N_r b\, i\mu_0 \omega N_t I a \int_0^\infty J_1(\lambda a) J_1(\lambda b) d\lambda \phi \qquad (6)$$

$$V^{soil} = \pi N_r b\, i\mu_0 \omega N_t I a \int_0^\infty \frac{\mu_{soil} u_o - \mu_o u_1}{\mu_{soil} u_o + \mu_o u_1} J_1(\lambda a) J_1(\lambda \rho) e^{-2u_o h} d\lambda \hat{\phi} \qquad (7)$$

Where:

$u_o{}^2 = \lambda^2 + k_o{}^2,\ u_1{}^2 = \lambda^2 + k_1{}^2$

$k_o{}^2$=0 (In the quasi static domain)

$k_1{}^2 = i\sigma_{soil}\mu_{soil}\omega$ (In the quasi static domain)

$\mu_0\ is\ magnetic\ permability\ of\ free\ space = 4x10^{-7}\frac{H}{m}$

$\mu_{soil} = magnetic\ permability\ of\ suelo\ (H/m)$

$\omega = Frequency\ of\ current\ flowing\ through\ the\ trajnsmitter\ \left(\frac{Rad}{s}\right)$

$J_1(x) = Bessel\ functions\ of\ the\ first\ kind\ and\ first\ order$

$a = Coil\ transmitter\ radius\ (m)$

$b = Coil\ receiver\ radius\ (m)$

$I = Curren\ amplitude\ (A)$

$N_t = Number\ of\ turns\ in\ the\ transmitter\ coil$

$\lambda = Integration\ variable$

2) Induced Voltage in the Receiver by a Metallic Buried Object:

Under this approximation, the buried object is replaced with an equivalent magnetic dipole and a current dipole and the principle of reciprocity is used to obtain the induced voltage, by this way (V^{target}) is calculated using the equivalent magnetic and current dipole moments $\overrightarrow{M}$ and $\overrightarrow{P}$ [7]

$$V^{target} = i\omega\mu_0 \vec{H}_1^b \cdot \vec{M} + E_1^b \cdot \vec{P} \quad (8)$$

Where E_1^b *y* $\vec{H}_1^b$ are the electric and magnetic field intensities that would be produced in the soil at the location of the equivalent dipole, if a unit of current would flow through the receiver coil. $\overrightarrow{M}$ and $\vec{P}$ depend on the shape of the buried object. $\overrightarrow{M}$ and $\vec{P}$ expressions depend on the induced fields produced by the current that flows through the receiver coil, on the dispersing object (its geometry and material properties ($\mu_2, \sigma_2, \epsilon_2$)) and on the soil properties ($\mu_1, \sigma_1, \epsilon_1$).

Because an expression for $\overrightarrow{M}$ and $\vec{P}$ is not easy to get for all shapes, the buried target is approximated by a sphere, which expressions for $\overrightarrow{M}$ and $\vec{P}$ are easily found in the literature. For a sphere with radius R, and with electromagnetic properties ($\mu_{target}, \sigma_{target}, \epsilon_{target}$) buried in soil with properties ($\mu_{soil}, \sigma_{soil}, \epsilon_{soil}$), the expression $\vec{M}$ y $\vec{P}$ are found on [7] and [3].

B. Numerical Modeling of Metal Detectors

The response of buried objects has been modeled numerically using techniques such as finite-difference, finite elements, and the integral method. The modeling of the electromagnetic induction problem should satisfy three criteria [12]: Capability to model buried objects arbitrarily, capability to model high contrast between the electromagnetic properties of the soil and buried objects and high computational efficiency. The method of Integral Equation of Volume and its variations is fast however; the maximum contrast allowed by this method is 300:1. The finite-differences method can model high contrasts (around 10^5:1) but, it does not allow the modeling of complex shapes. The finite-element method allows contrasts greater than 10^5:1, and allows flexibility to model complex shapes [9]. This method is similar to the Finite-difference Method [2] in the execution speed and the storage requirement.

Most of the developed models are able to model objects with arbitrary conductivity but constant permeability. In the case of FEM, it is easier to solve the linear system if it is assumed that permeability is constant over the entire scenario because variable permeability produces ill conditioned matrices.

C. Modeling of Metal Detectors Using the Finite Element Method

Although Maxwell equations can be directly solved in terms of electrical field (E) and magnetic field (H) using the finite element method, it is necessary to use penalty functions or to make an edge-based formulation to avoid spurious modes. A good alternative to avoid spurious modes is solving Maxwell equations formulated as a coupled potentials (A, V) system [6] given that the potentials are continuous in materials interfaces.

1) Potentials Formulation of Maxwell Equations:

Magnetic field density (B) and electric field (E) can be written in terms of magnetic vector potential (A) and scalar electric potential (V) as:

$$B(\omega) = \nabla \times A(\omega) \quad (9)$$

$$E = -(i\omega A + \nabla V) \quad (10)$$

As $B = \mu H$ equation (5) becomes:

$$\nabla \times B(\omega) = \mu\left(J_P(\omega) + \sigma E(\omega)\right) \quad (11)$$

Using the expression of reluctivity $\upsilon = \frac{1}{\mu}$ and substituting potentials equations in (11)

$$\frac{1}{\upsilon}\nabla \times \nabla \times A(\omega) + i\omega\sigma A + \sigma\nabla V = J_P(\omega) \quad (12)$$

In magnetoquasistatic approximation, current density (J=σE) is divergence free [14], therefore:

$$\nabla \cdot (\sigma E) = 0 \quad (13)$$

Replacing equation **(** 10) in the previous equation:

$$-\nabla \cdot [i\omega\sigma A + \sigma\nabla V] = 0 \quad (14)$$

Equations (12) and (14) are known as the Ungauged Curl-Curl coupled potential formulation of Maxwell equations.

2) Solution of the Ungauged Curl-Curl Formulation:

A solution of the Ungauged Curl-Curl formulation was proposed by [9] using secondary potential to avoid discretizing the transmitter coil [5] obtaining the following equations system:

$$-\nabla\cdot(i\omega\sigma A_s+\sigma\nabla V_s)=\nabla\cdot\left(i\omega\sigma_s A_p+\sigma_s\nabla V_p\right) \quad (15)$$

$$\upsilon\nabla\times\nabla\times A_s+i\omega\sigma A_s+\sigma\nabla V_s=-\upsilon_s\nabla\times\nabla\times A_p-i\omega\sigma_s A_p-\sigma_s\nabla V_p \quad (16)$$

Where A_s and V_s are secondary potentials (magnetic vector potential, and scalar electric potential induced by buried objects respectively), σ_s and υ_s are conductivity and reluctivity of buried objects. A_p and V_p are primary potentials (magnetic vector potential, and scalar electric potential induced by the transmitter coil over a half space), σ_p and υ_p are electrical conductivity of the soil or the air at the respective position, $\sigma=\sigma_p+\sigma_s$ and $\upsilon=\upsilon_s+\upsilon_p$. These primary potential can be found on [13].

The solution of the *Ungauged Curl-Curl* formulation using the traditional node based finite element method results in an ill conditioned left hand side of the linear system [9]. A good alternative for this is to use the edge-based FEM method. On [9] a mixed formulation, is proposed which describes A_s as a linear combination of edge basis functions (α_j) and V_s as a linear combination of node basis functions (φ_j).

$$A_s(x,y,z)=\sum_{j=1}^{M}A_{s_j}\alpha_j(x,y,z) \quad (17)$$

$$V_s(x,y,z)=\sum_{j=1}^{N}V_{sj}\varphi_j(x,y,z) \quad (18)$$

Where M is the number of edges and N is the number of nodes. Under this method A_{s_j} is a magnetic vector potential tangential to the edge *j*, and V_{sj} is the electric potential at the node *j*.

Replacing (17) and (18) in (15) and (16), applying Galerkin's method and Green function to reduce the differentiation order, the following linear system is obtained:

$$\sum_{j=1}^{M}\left(\upsilon A_{s_j}\left(\nabla\times\alpha_i(x,y,z),\nabla\times\alpha_j(x,y,z)\right)_V+A_{s_j}\left(\alpha_i(x,y,z),i\omega\sigma\left(\alpha_j(x,y,z)\right)\right)_V\right)+\sum_{k=1}^{N}V_{sk}\left(\alpha_i(x,y,z),\sigma\nabla\varphi_k\right)_V=-\left(\nabla\times\alpha_i(x,y,z),\upsilon_s B_p\right)_V+\left(\alpha_i(x,y,z),\sigma_s E_p\right)_V \quad (19)$$

$$\sum_{j=1}^{M}A_{s_j}\left(i\omega\sigma\nabla\varphi_i,\alpha_j(x,y,z)\right)_V+\sum_{k=1}^{N}V_{sk}\left(\nabla\varphi_i,\sigma\nabla\varphi_k\right)_V=-\left(\sigma_s\nabla\varphi_i,E_p\right)_V \quad (20)$$

This is a linear system that can be solved using the Quasi Minimal Residual (QMR) method with a Jacobi pre-conditioner. The right hand side of the linear system can be solved by using Gaussian Quadrature method [14] or the integration method proposed on [15], and the inner products can be calculated with the expressions found on [16] , [17] or [18].

III. RESULTS

A. Experimental Validation of the Model

In order to validate the model against laboratory measurements, a continuous wave metal detector prototype was built using a signal generator, a National Instruments PXI platform with oscilloscope module, a set of coils (transmitter and receiver) an automatic positioning system and a humus soil container.

TABLE I
Prototype Characteristics

Transmitter coil radius (m)	0.14
Receiver coil radius (m)	0.06
Frequency (KHz)	357
Current amplitude (A)	0.006

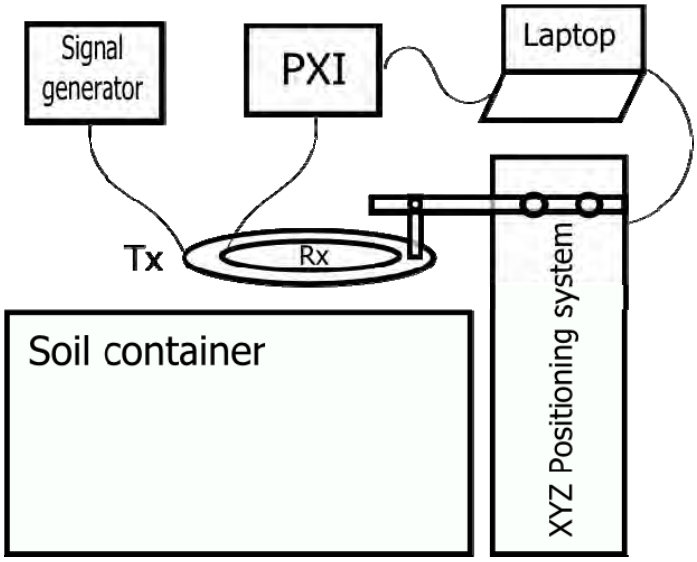

Fig 4. Continuous wave metal detector prototype

This prototype allows measuring the magnitude of induced voltage in the receiver coil by the transmitter (V_{air}), by the soil (V_{soil}) and by the buried object (V_{target}). In this case the buried object is an aluminum cube (5cm x 5cm x 5cm).

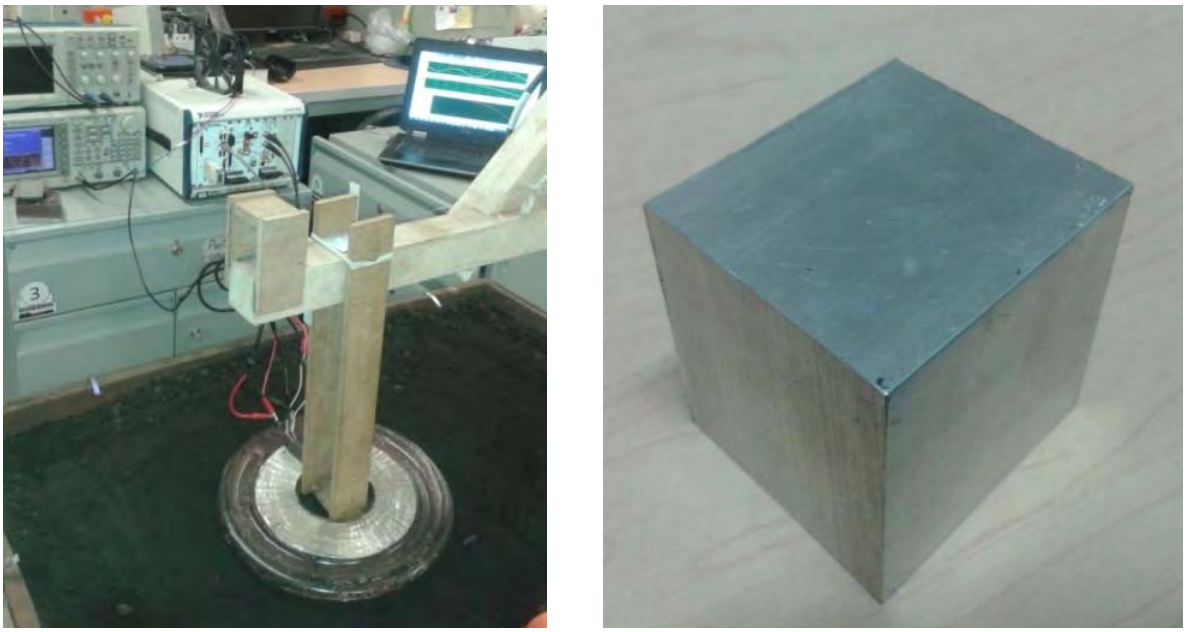

Fig 5. Laboratory prototype

The following figure shows V_{target} obtained experimentally (-) and V_{target} obtained simulating the same scenario (*), the figure shows close agreement between experimental and simulated data. Supported by this analysis, the numerical model can be used to simulate demining scenarios with high metallic content landmines.

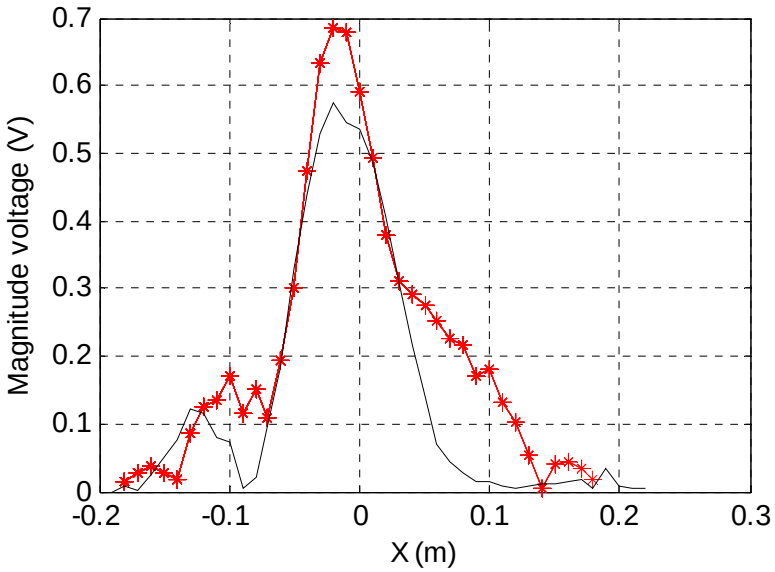

Fig 6. V_{target}, experimental (-) and simulated (*) results

B. Typical Demining Scenario Simulation Using the Analytical Model

In order to clearly observe the working principle of a continuous wave metal detector, a typical demining scenario was simulated, varying diverse parameters of the system:

Table II
Typical Demining Scenario Configuration

Transmitter and receiver height (m)	0.02
Transmitter coil radius (m)	0.1
Receiver coil radius (m)	0.1
Soil conductivity (S/m)	0.001
Soil susceptibility	0
Sphere depth (m)	0.1
Sphere radius (m)	0.005
Sphere conductivity (S/m)	3.54×10^7
Sphere relative permeability	1
Product NtNrI	1

Fig 7 shows simulation results of the typical scenario, when distance between the vertical axis of coils and buried object location varies. V_{total} is the sum of all voltages induced in the receiver ($V_{total}= V_{air}+V_{soil}+V_{target}$) and it is the voltage that a receiver would measure in the experimental case.

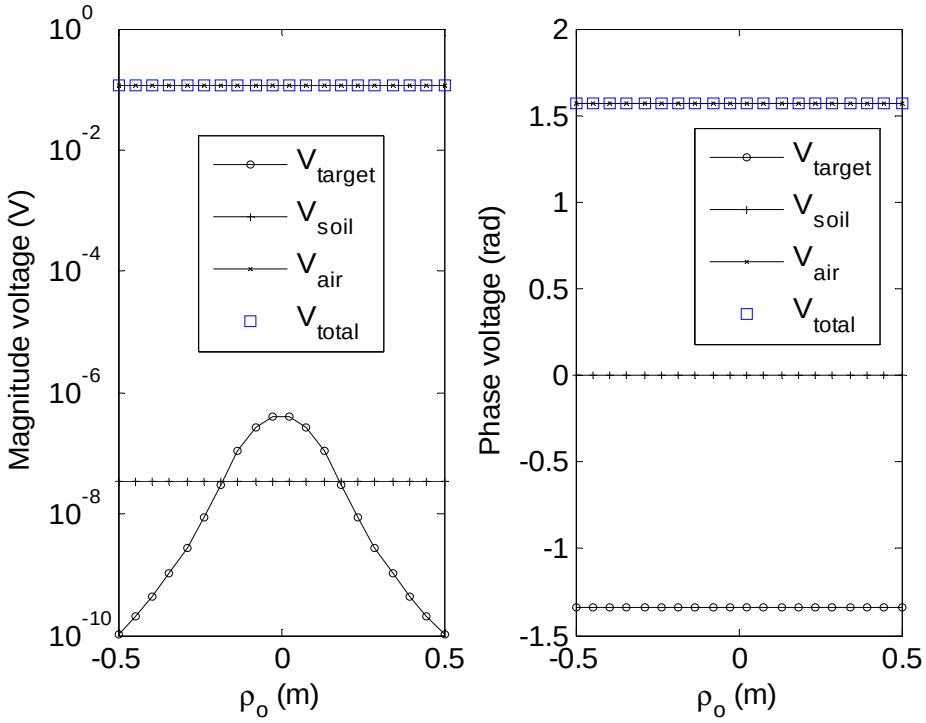

Fig 7. Distance from loops axis ($\boldsymbol{\rho_o}$) vs Induced voltage

The voltage induced directly by the loop transmitter in the receptor (V_{air}) is much higher than the voltage induced by the buried object, and thus V_{total} is equivalent to V_{air}. Therefore, changes in phase or magnitude due to the buried object are not noticeable. Because of this it is necessary to recognize and remove the value V_{air} during the design and construction processes of metal detectors. Removing V_{air} yields $V_{total}= V_{soil}+V_{target}$ and the new V_{total} curve is shown in Fig 8.

Fig 8 illustrates that as the detector approaches the buried object (reducing ρ_o), the change in magnitude and phase of induced voltage becomes larger, and the maximum change is obtained when ρ_o is equal to zero. In this scenario, the magnitude becomes twelve times larger and the change in phase is 1.26 rad or 72.22 deg.

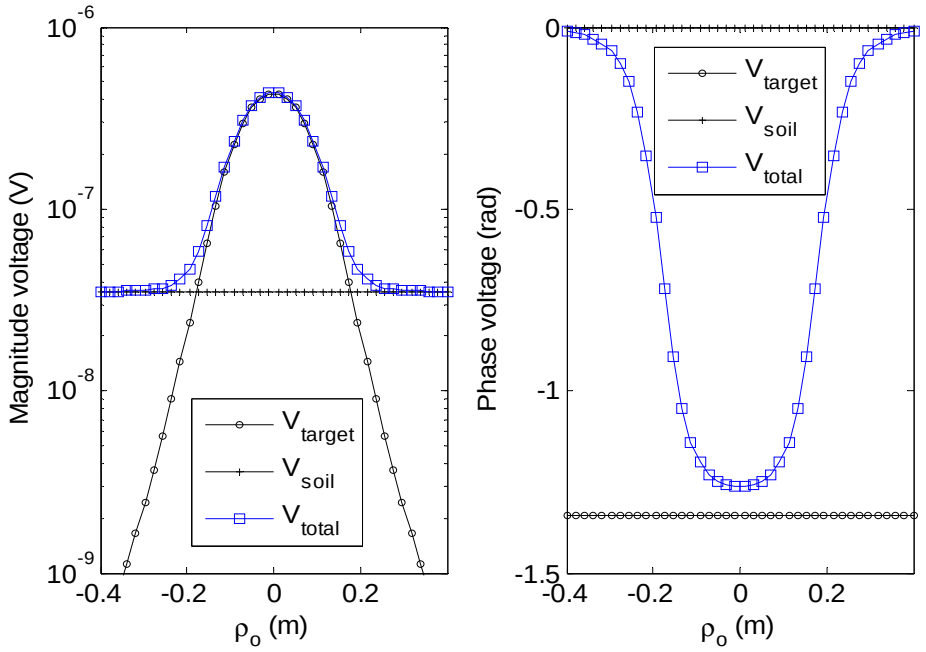

Fig 8. Distance from loops axis vs Induced voltage ($V_{total}=V_{target}+V_{soil}$)

Next, the results are shown of simulating the typical demining scenario varying the properties of the detector, the buried object and the soil. For each case, ρ_o=0.

1) Effect of Varying the Detector Properties:

Fig 9 shows the behavior of induced voltage as a function of frequency. From the graphic of magnitude in Fig 9 it is observable that frequency does not affect the difference between V_{soil} and V_{total}, therefore, if the detector only measures the magnitude of the voltage to detect a target, the buried object has the same possibility of being detected under any frequency. However, the phase is widely influenced by frequency, and as the frequency increases the difference between V_{soil} and V_{total} increases also, until the frequency equals approximately 50 KHz. At subsequently higher frequencies the difference becomes constant.

Fig 10 and Fig 11 represent the induced voltage as a function of transmitter and receiver coil radius respectively, showing that the magnitudes of V_{soil} and V_{target} depend on the size of both coils. The best probability of detection is obtained when the difference between V_{target} and V_{soil} is at a maximum. In this case the best probability of detection is obtained with a transmitter coil radius of approximately 7 cm. When transmitter coil radius is greater than 50 cm, V_{soil} predominates over V_{target}, therefore making the buried object undetectable. With regards to the phase of the induced voltage it is clear that the phase of V_{target} predominates over the phase of V_{soil} when transmitter coil radius is smaller than 10 cm. As the transmitter coil radius increases this makes object detection increasingly difficult.

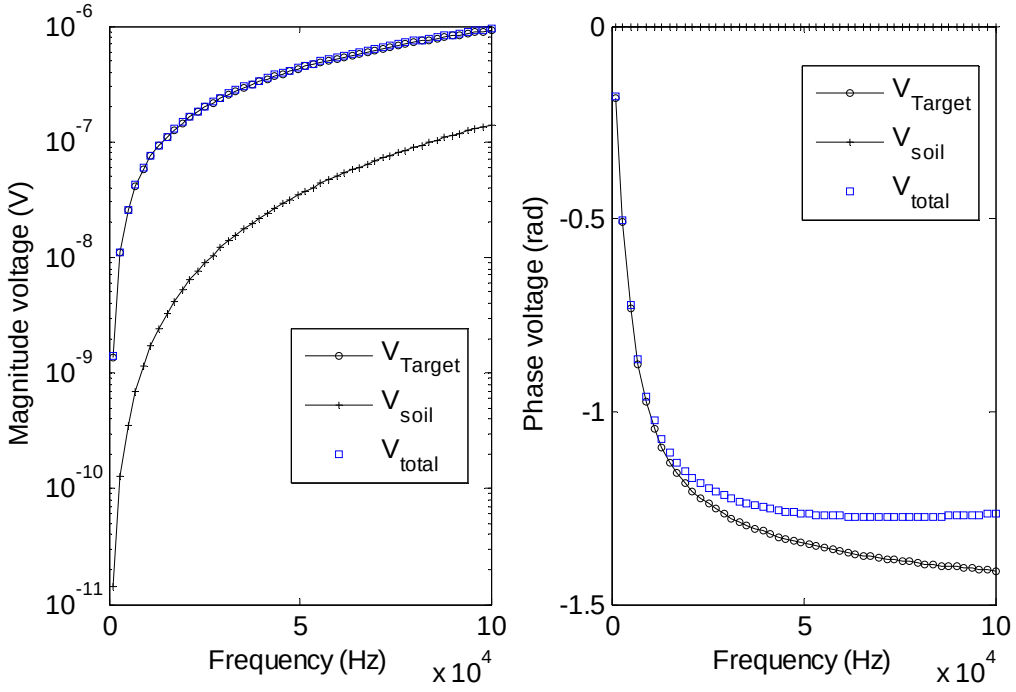

Fig 9. Frequency vs Induced voltage

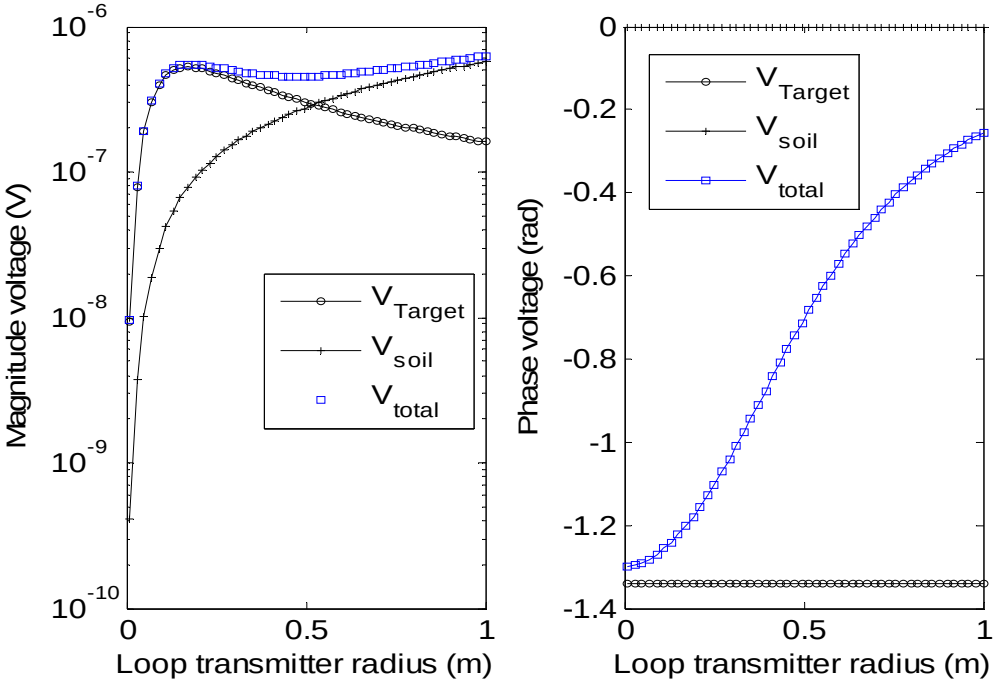

Fig 10. Transmitter coil radius vs Induced voltage ($V_{total}=V_{target}+V_{soil}$)

Given Fig 11 it is logical to conclude that the analysis for receiver coil radius is equivalent to that of the transmitter.

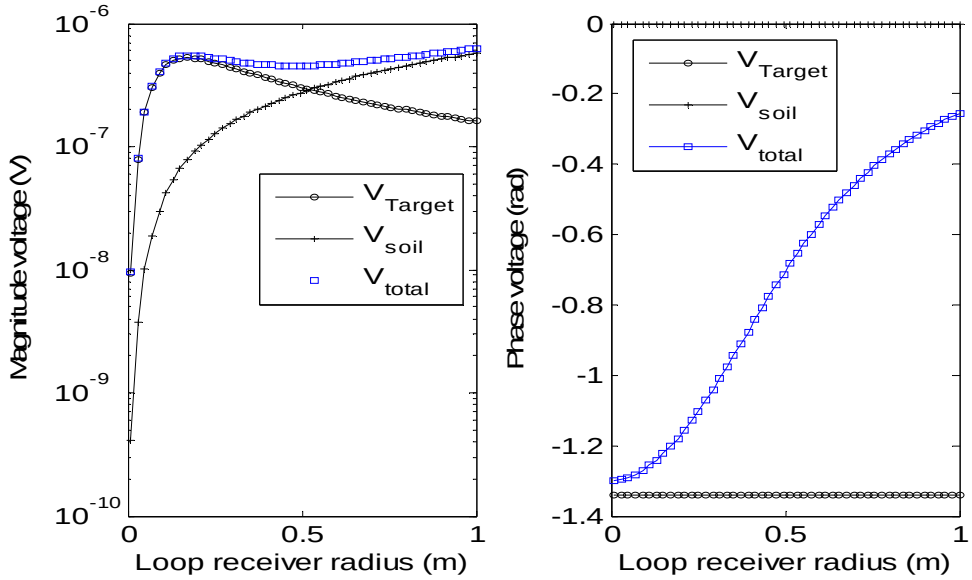

Fig 11. Receiver coil radius vs Induced voltage (Vtotal=Vtarget+Vsoil)

2) Effect of Varying the Metal Properties:

Fig 12 presents induced voltages as a function of buried sphere electrical conductivity. It is clear that as conductivity increases, the magnitude and change of phase of induced voltages increase too. For a metallic sphere with electrical conductivity over $1x10^5$ S/m the magnitude of V_{target} is approximately ten times larger than the magnitude of V_{soil}. For objects with greater conductivity, the magnitude of V_{target} does not change significantly. A potential conclusion from this is that there is saturation that there is a saturation phenomenon of the magnitude of V_{target} while target conductivity is increasing. According to this it is not possible to discriminate kinds of metals by measuring the magnitude of V_{total} or V_{target}.

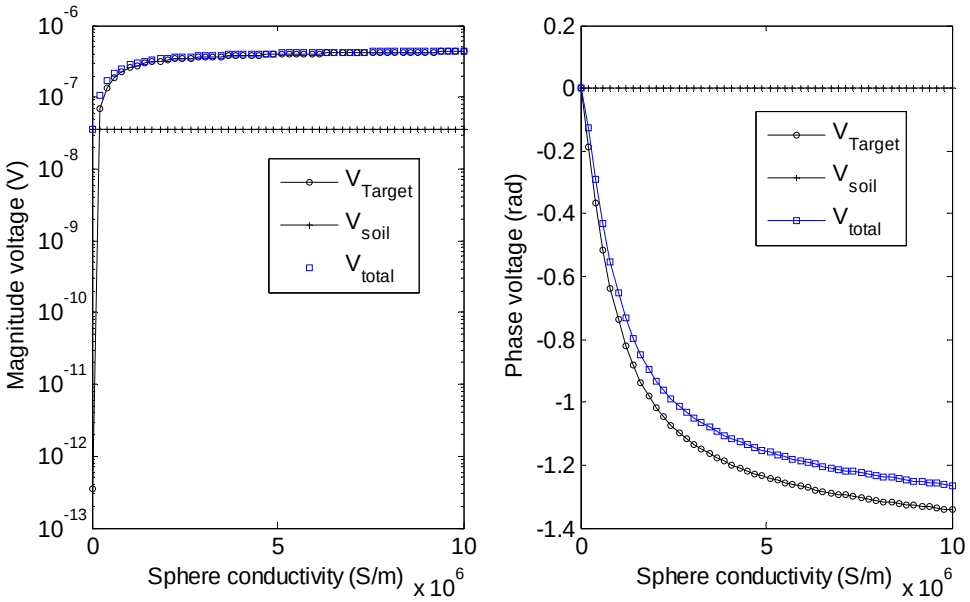

Fig 12. Sphere conductivity vs Induced voltage (Vtotal=Vtarget+Vsoil)

Fig 13 presents induced voltage as a function of sphere relative permeability. This figure suggests that permeability is not highly influential in the magnitude of V_{target} but is highly influential in the phase of V_{target}. According to the phase graph, a sphere with relative permeability close to 1 induces a voltage waveform lagging the current waveform. Whereas a sphere with relative permeability much greater than 1 induces a voltage leading the current by approximately 90°.

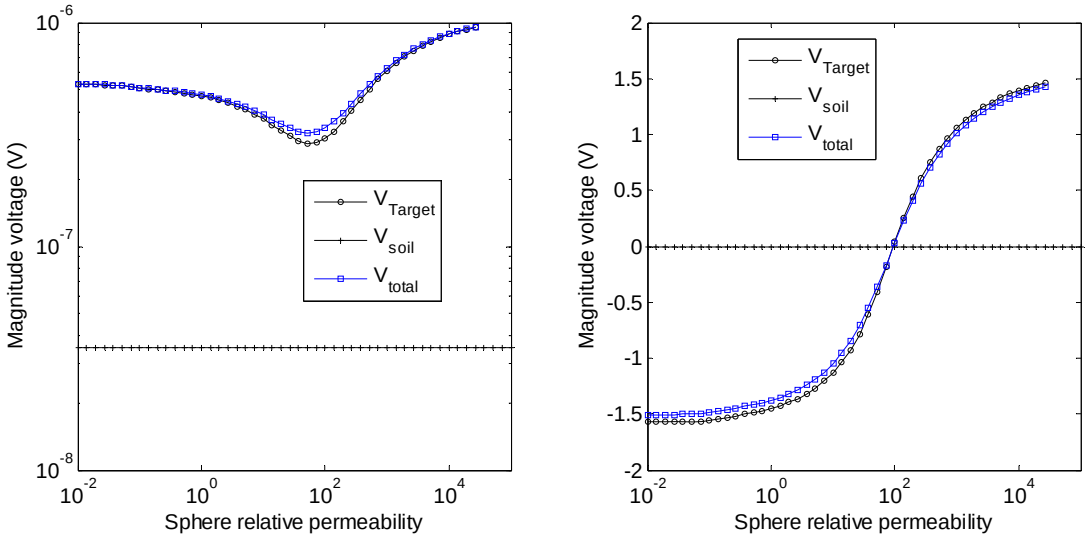

Fig 13. Sphere relative permeability vs Induced voltage (Vtotal=Vtarget+Vsoil)

Fig 14 shows induced voltages as a function of the sphere radius. In this case it is clear that the larger the radius is, the higher the magnitude of voltage is, and the phase delay increases until it reaches its maximum value of -90°.

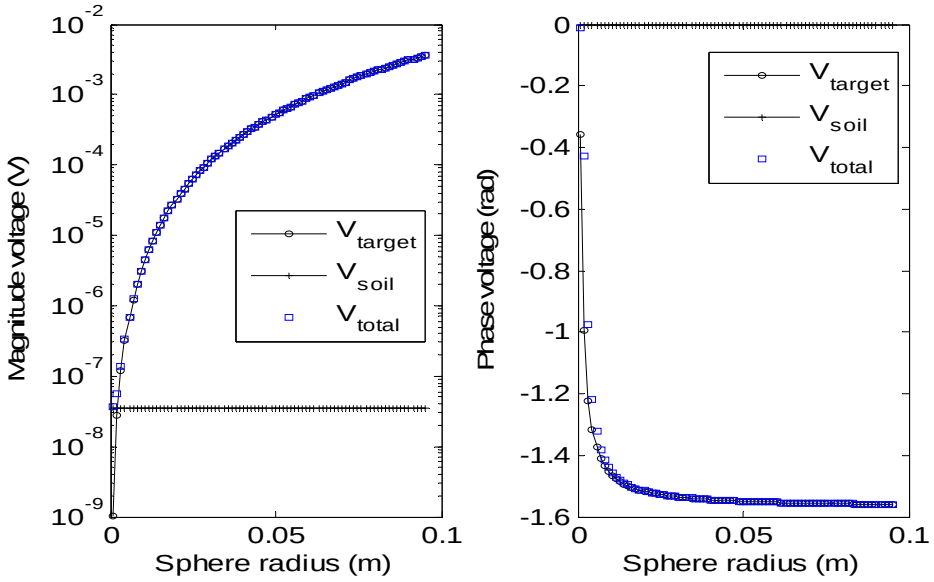

Fig 14. Sphere radius vs Induced voltage (Vtotal=Vtarget+Vsoil)

3) Effect of Varying the Soil Properties:

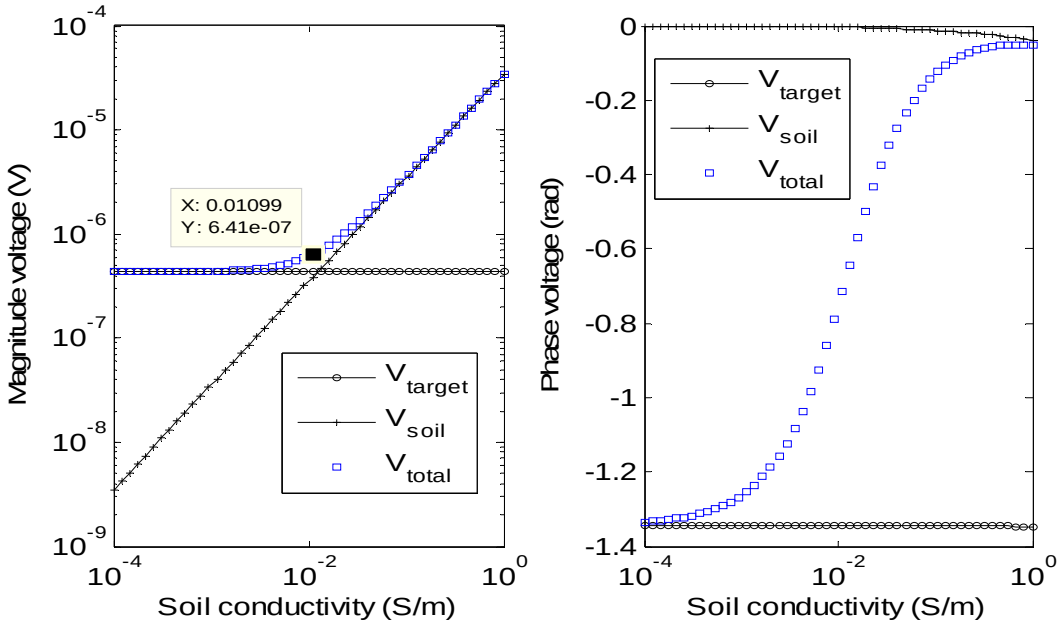

Fig **15** shows the influence of soil electrical conductivity on induced voltages. In a typical demining scenario with a buried object located 10 cm under the surface, a high conductivity soil can make the object impossible to detect when the magnitude or phase of V_{total} is being analyzed. In this case for both measures (magnitude and phase) the object is impossible to detect when soil has conductivity higher than 0.01 S/m. It can be seen also that the magnitude and phase of V_{target} does not change significantly when soil conductivity changes.

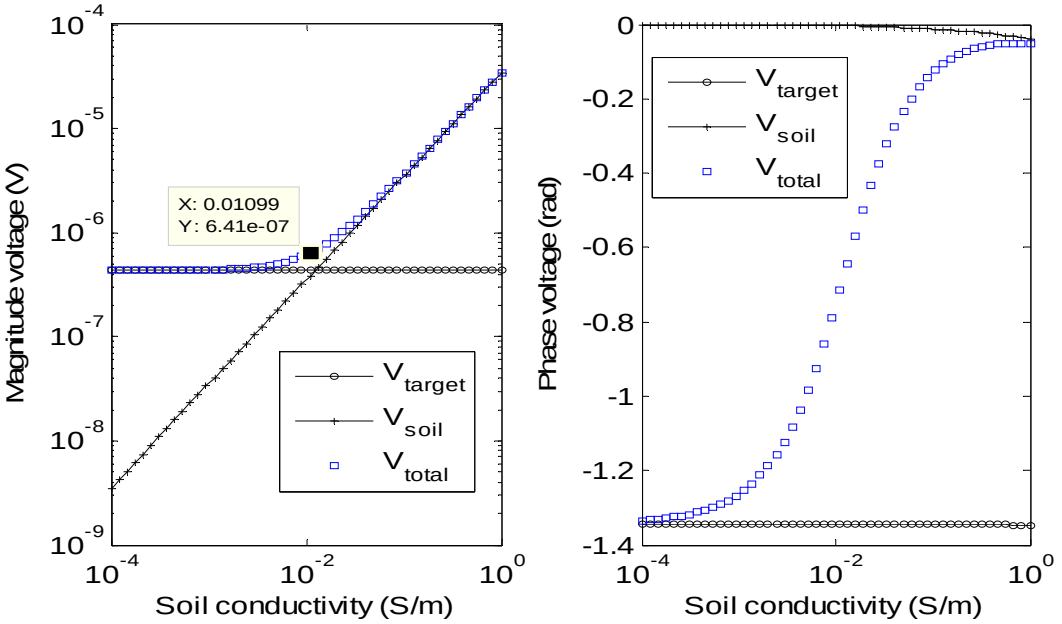

Fig 15. Soil conductivity vs Induced voltage (Vtotal=Vtarget+Vsoil)

Fig 16 shows the effect of changing soil magnetic susceptibility on induced voltages. The magnitude V_{soil} is at a minimum when soil magnetic susceptibility is zero, in this case, $|V_{total}|=|V_{target}|$. However, small changes in soil susceptibility can make $|V_{total}|=|V_{soil}|$ and the buried object impossible to detect. In this particular case, the target is undetectable when soil susceptibility is smaller than $-1x10^{-5}$ or higher than $4x10^{-5}$. Similarly for phase, and only when susceptibility is very close to zero, the phase of V_{target} predominates over the phase of V_{soil}. In this particular case if soil susceptibility is greater than $1x10^{-4}$ or smaller than $-6x10^{-5}$, the phase of V_{total} is equal to the phase of V_{soil} and the buried target cannot be detected.

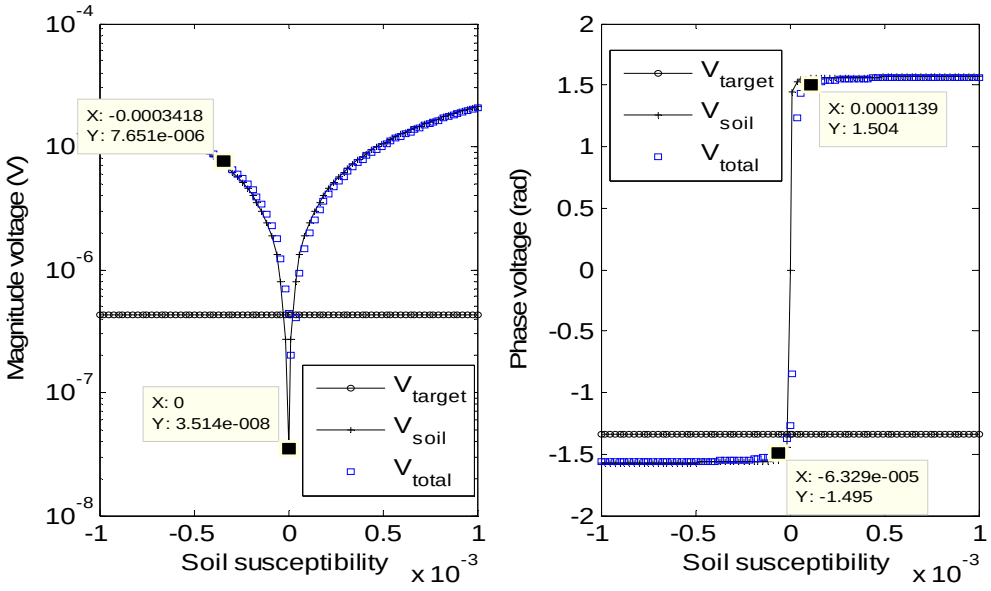

Fig 16. Soil magnetic susceptibility vs Induced voltage (Vtotal=Vtarget+Vsoil)

IV. CONCLUSIONS

The results of the numerical model were validated against laboratory measurements of a prototype of a continuous wave's metal detector which allows measuring the magnitude of the induced voltage. The results fit well therefore that model can be applied to mine detection scenarios, when the landmines include high metallic content like shrapnel

The analytical model presented is less flexible than numerical techniques; nevertheless, it is a valuable tool to observe the metal detectors operation´s principle and get results in a rapid fashion.

The voltage induced directly by the loop transmitter in the receptor is generally higher than the voltage induced by the buried object therefore; the changes in the phase and magnitude of the voltage in the presence of a metal are not significant. It is very important to remove this value, using electronic techniques or software.

When a metal detector of concentric loops is directly over the buried object, it obtains the maximum change in magnitude and phase of the induced voltage. In a typical scenario of detection, magnitude of voltage can be a hundred times higher and the change in phase can be up to 90°.

As the frequency increases, the magnitude of induced voltages increases also.

If the detector only measures the magnitude of the voltage to detect a target, the buried object has the same possibility of being detected under any frequency. However, the phase is widely influenced by frequency.

The maximum magnitude of the induced voltage by the buried object depends on the size of the transmitter and receiver loops. As the transmitter or receiver coil radius increases this makes landmines detection increasingly difficult.

The magnitude and phase of induced voltage by a small buried object does not change significantly when soil conductivity changes.

It is not considered possible to discriminate the metal type with a CW metal detector measuring magnitude of voltage when metal permeability is equivalent.

A highly conductive soil can make the object impossible to detect, when the magnitude or phase of V_{total} is being analyzed.

Small changes in the magnetic susceptibility of the soil significantly affect the performance of a detector which can generate false alarms if measuring the magnitude of the induced voltage, or the object cannot be detected when measuring the phase.

REFERENCES

[1] K. Takahashi, H. Preetz and J. Igel, "Soil properties and performance of landmine detection by metal detector and ground-penetrating radar—soil characterisation and its verification by a field test," Journal of Applied Geophysics, vol. 73, pp. 368-377, 2011.

[2] J. L. Stalnaker, M. E. Everett, A. Benavides and C. J. Pierce Jr., "Mutual Induction and the Effect of Host Conductivity on the EM Induction Response of Buried Plate Targets Using 3-D Finite-Element Analysis," IEEE Transactions on Geoscience and Remote Sensing, vol. 44, no. 2, February 2006.

[3] Y. Das, "Effects of Soil Electromagnetic Properties on Metal Detectors," IEEE Transactions on Geoscience and Remote Sensing, vol. 44, no. 6, pp. 1444-1453, Junio 2006.

[4] D. Pridmore, G. Hohmann, S. Ward and W. Sill, "An investigation of finite-element modeling for electrical and electromagnetic data in three dimensions," Geophysics, vol. 46, p. 1009–1024, 1981.

[5] E. A. Badea, M. E. Everett, G. A. Newman and O. Biro, "Finite-Element Analysis of Controlled-Source Electromagnetic Induction Using Coulomb-Gauged Potentials," Geophysics , vol. 66, no. 3, pp. 786-799, May-June 2001.

[6] J. Stalnaker, "A finite element approach to the 3D CSEM modeling problem and applications to the study of the effect of target interaction and topography". Doctoral dissertation, Texas A&M University, Texas A&M University, 2004.

[7] Y. Das, "A Preliminary Investigation of the Efects of Soil Electromagnetic Properties on Metal Detectors," Proc. SPIE, p. 677–690, 2004.

[8] C. Bruschini, "On the low-frequency EMI response of coincident loops over a conductive and permeable soil and corresponding background reduction schemes," Geoscience and Remote Sensing, IEEE Transactions on, vol. 42, no. 8, pp. 1706-1719, 2004.

[9] S. Mukherjee, "Three dimensional controlled-source electromagnetic Edge-based finite element modeling of conductive and permeable heterogeneities," College Station, 2010.

[10] T. G. I. C. f. H. D. GICHD, "Detectors and Personal Protective Equipment Catalogue 2009," Geneva, 2009.

[11] F. I. Zyserman, "Simulación numérica de difusión electromagnética en el subsuelo terrestre" (Tesis de doctorado), 2000.

[12] S. Mukherjee and M. E. Everett, "3D controlled-source electromagnetic edge-based finite element modeling," GEOPHYSICS, vol. 76, no. 4, p. F215–F226, 2011.

[13] S. H. Ward and G. W. Hohmann," Electromagnetic theory for geophysical applications: Electromagnetic Methods in Applied Geophysics", M. N. Nabighian, Ed., Investigations in Geophysics, 1988, pp. 131-311.

[14] J.-M. Jin and J. Jin, "The finite element method in electromagnetics", Wiley New York, 2002.

[15] M. A. Eisenberg and L. E. Malvern, "On finite element integration in natural co-ordinates," International Journal for Numerical Methods in Engineering, vol. 7, no. 4, pp. 574-575, 1973.

[16] J. Velımský, "Electromagnetic induction in a heterogeneous Earth's mantle: Time-domain modelling", Ph. D. thesis, Faculty of Mathematics and Physics, Charles University, 2003.

[17] C. Pozrikidis, "Introduction to finite and spectral element methods using Matlab", 2005.

[18] C. Reddy, M. D. Deshpande, C. Cockrell and F. B. Beck, "Finite element method for eigenvalue problems in electromagnetics", National Aeronautics and Space Administration, Langley Research Center, 1994.

[19] J. McNeill, "Applications of transient electromagnetic techniques", Geonics Limited, 1980.

[20] D. B. Davidson, "Computational electromagnetics for RF and microwave engineering", New York: Cambridge University Press, 2005.

[21] J. Larsson, "Electromagnetics from a quasistatic perspective," American Journal of Physics, vol. 75, pp. 230-239, 2007.